Transition Metal Complexes with Appended Benzimidazole Groups for Sensing Dihydrogenphosphate

Chloe L. Howells, Andrew J. Stocker, Joshua N. Lea, Nathan R. Halcovitch, Humaira Patel and Nicholas C. Fletcher*

Department of Chemistry Lancaster University, Bailrigg, Lancaster, LA1 4YB, UK.

Lancaster University

Bailrigg, Lancaster, LA1 4YB, UK

E-mail: n.fletcher@lancaster.ac.uk

Abstract: Four new complexes [Ru(bpy)₂(bbib)](PF₆)₂, [Ru(phen)₂(bbib)](PF₆)₂, $[Re(CO)_3(bbib)(py)](PF_6)$ and $[Ir(ppy)_2(bbib)](PF_6)$ [where bbib = 4,4'-bis(benzimidazol-2-yl)-2,2'bipyridine] have been prepared and their photophysical properties determined. Their behaviour has been studied with a variety of anions in acetonitrile, DMSO and 10% aguated DMSO. Acetate and dihydrogenphosphate demonstrate a redshift in the bbib ligand associated absorptions suggesting that the ligand is strongly interacting with these anions. The ³MLCT emissive state is sensitive to the introduction of small quantities of anion (sub-stoichiometric quantities) and significant quenching is typically observed with acetate, although this is less pronounced in the presence of water. The emissive behaviour with dihydrogenphosphate is variable, showing systematic changes as anion concentration increases with several distinct interactions evident . ¹H NMR and ³¹P NMR titrations in a 10% D₂O – D₆-DMSO mixture suggest that with dihydrogenphosphate, the imidazole group is able to act as both a proton acceptor and donor. It appears that all four complexes can form a {[complex]₂-H₂PO₄} "dimer", a one-to-one species (which the X-ray crystallography study suggests is dimeric in the solid-state), and a complex with a combined bis(dihydrogenphosphate) complex anion. The speciation relies on complex equilibria dependent on several factors including the complex charge, the hydrophobicity of the associated ligands, and the solvent.

Introduction

The selective recognition of anions has developed over the last two decades into a vibrant area of supramolecular chemistry, and is now beginning to find application within a number of fields. There is an increasing variety of molecular architectures and binding modes available to tailor both selectivity and application, including the use of halogen bonding and anion— π interactions. By far the most common approach has been the use of directional hydrogen-bonding, using hydroxyl, urea, thiourea and guanidium units, to tune the anion recognition and selectivity. Compounds bearing pyrroles, imidazoles, triazoles and imidazolium moieties have recently been shown to provide considerable anion specificity.

The recognition of phosphate by artificial receptors remains a considerable challenge though, [14] although study is driven forward by its ubiquitous role within living systems. [15] There is a delicate interplay between protonation and electrostatics that enable it to be a reactive intermediate, and yet possess a remarkably stable tetrahedral geometry. The biological behaviour appears to be activated by the relationship between the charge and its local environment, leading to a number of possible recognition strategies. [12,16] Whilst many studies have been completed using dihydrogenphosphate, speciation between condensed species such as pyrophosphate and biologically important phosphates such as ATP^[18] remains an active area of research, and the detection of organophosphates opens new opportunities to sense^[19] and even deactivate "nerve agents". [20]

The detection of environmental phosphates is complicated though by the high hydration enthalpy (ΔG_{hyd} of H_2PO_4^- approx. -465 kJ mol^{-1})^[21] making coordination particularly challenging in aqueous environments. ^[22] A variety of ingenious strategies have been considered to overcome this including host "preorganization" and "encapsulation". ^[23] The issue is further complicated by the degree of protonation of the phosphate unit. In a biological or environmental setting, it typically presents as an equilibrium of the monovalent H_2PO_4^- and the divalent HPO_4^{2-} forms. In addition, hydrogenphosphate readily forms dimers and oligomers in solution through "anti–electrostatic" hydrogen bonds, ^[24] which can lead to large anionic systems, particularly in the presence of urea. ^[25]

In our earlier studies, we have shown that linear thiourea bridged 2,2'-bipyridine ligands have good affinity towards both acetate and phosphate, and these can be enhanced by coordination of the ligand to neutral rhenium(I) fluorophores. [26] We proposed that each thiourea unit binds, not one, but two dihydrogenphosphate anions cooperatively with the first binding coefficient being smaller than the second, suggesting that a proton transfer is commensurate with the anion recognition in acetonitrile.

The development of phosphate recognition has gone hand in hand with both fluorometric or colorimetric sensing. This requires a good electronic communication between the "binding unit" and an appropriate chromophore. [27] Fluorescent zinc complexes have shown considerable application in this respect, [28] using the direct coordination and bridging of the phosphate between two metal cations permitting good speciation. Similarly, lanthanide complexes have shown a considerable interaction with a range of species, [29] with speciation controlled by the steric control around the metal centre, and secondary functionalization providing opportunities to develop ATP selectivity. [30] The diimine complexes of ruthenium(II)[31] and rhenium(I),[31a,32] and more recently the cyclometalated complexes of iridium(III)[31b,32-33] have drawn much interest in the detection of phosphate. For example, a rhenium(I) tricarbonyl polypyridine with an imine functionalized phenol moiety can have a "turn-on" emissive response with a range of anions,[34] whilst an aminoethanol substituted 1,10-phenanthroline (phen) ruthenium complex has demonstrated an aggregation induced emission response. [35] And by exploiting selective hydrogen-bonding interactions, a phen bound sulfonamido system has shown recognition of fluoride, acetate, and dihydrogenphosphate. [36]

A component within many recent studies is an imidazole group, such as imidazo[4,5-f]-[1,10]phenanthroline which can be bonded to a variety of metals enabling a photophysical response. [37] The ligands 2,2-bisimidazole (biimH₂) and bibenzimidazole (bbiH₂), along with a number of related derivatives, show that they can coordinate directly to both {Ru(bpy)₂} or {Ir(ppy)₂}, [38] and the amino groups then form twofold second-sphere hydrogen bonds with various anions with a commensurate enhancement in the emission. In many instances, deprotonation appears to occur with acetate, fluoride and dihydrogenphosphate. In a related set of studies, a series of chelating N-bound pyridyl triazoles, again bound to either a {Ru(bpy)₂} or {Ir(ppy)₂} fluorophore, can elicit a more selective response to H₂PO₄^{-[39]} For example, using a ligand derived from pyrenylimidazole-10-pyridin-2-yl-9H-9,11-diazacyclopentapyrene, phosphorescence is enhanced by the addition of dihydrogenphosphate, but quenched with acetate and fluoride. [40] Selectivity can also be enhanced by the inclusion of an appended urea^[41] or even benzothiazole groups. [42] With these systems, it is also possible to exploit halogen bonding to enhance selectivity and avoid the possibility of deprotonation. [39d, 43] In similar studies a cyclometalated Ir(III) complex containing a methylene bridged benzimidazole substituted 1,2,3-triazole has demonstrated good photoluminescent detection of pyrophosphate. [44]

In our own studies, we have previously reported a series of ruthenium(II) polypyridyl complexes functionalized with benzothiazole or benzoxazole groups. [45] These were shown to bind to the minor groove of duplex DNA, with the optimum configuration for DNA interaction was found to be substitution with benzothiazoles at the 4 and 4'-positions of a 2,2'-bipyridine (bpy) chelate. Within the scope of these studies, we also explored the synthesis 4,4'-bis(benzimidazol-2-yl)-2,2'-bipyridine (bbib) and its subsequent coordination to ruthenium, [46] although the complexes proved to rather insoluble, and the interactions with DNA itself indistinct. In this report we revisit this ligand and explore its potential for selective dihydrogenphosphate recognition when bonded to a series of emissive metal centres. This study illustrates that the binding behaviour of phosphate with supramolecular hosts is far more intricate than previously thought, and illustrates new strategies that may work under ambient pH conditions.

Results and Discussion

Synthesis

A series of emissive metal complexes were prepared using standard literature procedures (Scheme 1). 4,4'-Dicarboxylic acid-2,2'-bipyridine was initially condensed with o-phenylenediamine using polyphosphoric acid as both solvent and dehydrating agent. Precipitation in basic aqueous solution resulted in 4,4'-bis(benzimidazole-2-yl)-2,2'-bipyridine (bbib) as a pale brown amorphous solid. The identity of the product was confirmed by ¹H NMR

spectroscopy in DMSO (Figure S1) and mass spectrometry. In the ¹H NMR spectrum, the signals attributed to the H³ on the pyridine ring are in a significantly downfield position at 9.3 ppm due to the proximity to the imidazole unit. The product is very insoluble in most common solvents, including DMSO preventing analysis by ¹³C NMR spectroscopy. However, crystals were grown by slow evaporation of a DMSO-D₆ solution, and the structure was confirmed via single crystal x-ray crystallography, indicating the ligand is a highly conjugated planar system (Figure S2).

Scheme 1. The complexes synthesis; conditions (a) (i) 1,2-diaminobenzene in polyphosphoric acid, 220 °C, 24 h, (ii) NaHCO₃ (aq), (b) (i) [Ru(bpy)Cl₂] or [Ru(phen)Cl₂], CF₃SO₃H, in ethylene glycol, (ii) KPF₆ (aq), (c) [Re(CO)₅Br] in DMSO, (e) (i) Ag(ClO₄) in pyridine (ii) KPF₆ (aq), (f) (i) [{Ir(ppy)₂(μ -Cl)}₂] in DMSO, (ii) KPF₆ (aq).

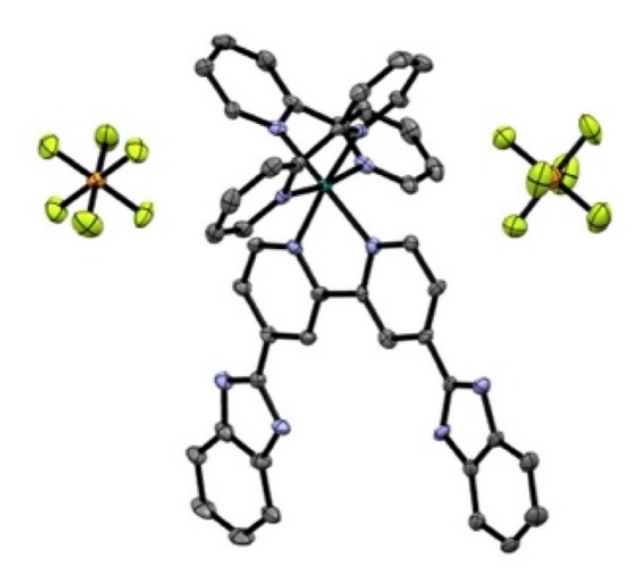


Figure 1 The X-ray structure of $[Ru(bpy)_2(bbib)](PF_6)_2$, units with ellipsoids at 50% probability and hydrogens omitted for clarity.

The ligand bbib was coordinated to ruthenium(II) by heating it with either $[Ru(bpy)_2Cl_2]$ or $[Ru(phen)_2Cl_2]$ in ethylene glycol with a small quantity of triflic acid to improve ligand solubility. These formed dark red solutions, and both $[Ru(bpy)_2(bbib)](PF_6)_2$ and $[Ru(phen)_2(bbib)](PF_6)_2$ were precipitated with the addition of an aqueous solution of potassium hexafluorophosphate. The resulting red complexes were purified by size exclusion chroma-tography (Sephadex® LH20) in 54

and 46 % yield respectively. The two products were characterized by ¹H NMR spectroscopy (Figure S3 & 4), and fully assigned via COSY and NOESY techniques. Consistent with the bbib ligand, the signal arising for the H³ proton adjacent to the imidazole function is observed to be significantly downfield at typically 9.6 ppm, and like the observed NH signal (typically at 12 to 14 ppm), was very susceptible to the presence of base. ^[47] Further there was notable broadening of the aromatic signals related to the benzimidazole function. The identity was further confirmed by mass spectrometry, with the two products identified from the corresponding divalent cation less the associated anions. Crystals of Ru(bpy)₂(bbib)](PF₆)₂ were grown from methanol by slow evaporation to give the racemic pair in the until cell, showing that the ligand retains a planar configuration when complexed (Figure 1).

The isolation of the rhenium(I) complexes proved challenging. The neutral complex [Re(bbib)(CO)₃Br] was obtained by prolonged heating of the ligand in DMSO, and realizing the complex by precipitation from water. This was characterized by ¹H NMR spectroscopy, resulting in very broad signals. However, the inclusion of one equivalent of tetrabutylammonium bromide in the solution resulted in the peaks sharpening significantly (Figure S5). This suggests that the bromide can dissociate and be replaced by the solvent (DMSO or acetonitrile). Electrospray mass spectrometry initially identified the product with the bromide substituted by the ambient solvent. However with the inclusion of a small quantity of a bromide salt, the protonated molecular ion could be detected. Subsequent removal of the bromide by silver salt precipitation, and replacement of the free site with pyridine and isolation as the hexafluorophosphate salt was easily achieved. confirmed by the identification of the molecular ion less the PF₆⁻ anion. The ¹H NMR spectrum though proved to be remarkably broad (Figure S6), particularly the aromatic benzimidazole peaks despite repeated attempts at further purification. On hearting the mixture to ~75 °C (Figure S7), the peaks resolved, and it is probable that there is either a relatively slow rotation around the bipyridine-imidazole bond, or a slow proton exchange across the imidazole function. Additionally, the pyridine showed inequivalence, indicating it adopts either an asymmetric orientation, or can partially exchange with the solvent.

The isolation of the iridium(III) complex $[Ir(ppy)_2(bbib)](PF_6)$ was realised through the reaction of $[\{Ir(ppy)_2(\mu-CI)\}_2]$ with bbib in a small amount of DMSO over 16 h. Purification by column chromatography indicated a number of products were present, with the final major band isolated in a disappointing 15%, proving to be the desired *trans* product, having C_2 symmetry as evidenced in the 1H NMR spectrum, and the molecular fragment for the complex cation less the PF_6^- anion. The 1H NMR spectrum again presents the bbib- H^3 signal in an unusual downfield position (10.7 ppm; Figure S8).

Photophyiscal Characterization

The UV / visible absorption spectra of [Ru(bpy)₂(bbib)](PF₆)₂ and [Ru(phen)₂(bbib)](PF₆)₂ consist of a number of well-defined bands in the range 200-550 nm (Table 1, Figure 2). These can be assigned by comparison to [Ru(bpy)₃]²⁺ and [Ru(phen)₃]²⁺; with both exhibiting the UV absorptions at 290 and 263 nm attributed to the ligand centred (LC) bpy and phen p-p* transition respectively. Both complexes also exhibit a broad absorption in the region of 350 nm consistent with the presence of a the bbib p-p* transition in keeping with the previously reported analogous thiazole and oxazole complexes. [45] The metal-to-ligand-charge-transfer (MLCT) $d \rightarrow p^*$ transitions appear to arise from a complex manifold of energy levels over the range from 400 to 550 nm, the longer wavelength transitions are assumed to be associated with the MLCT to the bbib ligand. The emission spectra of both complexes demonstrate a steady-state emission in aerobic solution at 645 and 638 nm when excited at 450 nm, and an enhanced quantum yield of 0.055 and 0.069 in comparison to $[Ru(bpy)_3](PF_6)_2$ ($\Phi_{em} = 0.040^{[48]}$), with the emission from the phenanthroline complex, as anticipated, being slightly greater. In comparison to the analogous oxazole and thiazole complexes [Ru(bpy)2-(bbob)](PF₆)₂ ($I_{max} = 673 \text{ nm}$, $\Phi_{em} = 0.013$) and [Ru(bpy)₂(bbtb)](PF₆)₂ ($I_{max} = 686 \text{ nm}$, $\Phi_{em} = 0.015$), the imidazole complex emission is blue shifted by 40 nm, and demonstrates a more emissive excited state, indicating that the change of the heterocyclic ring structure (NH compared to O or S) has a dramatic, and as yet unexplained, effect on the excited state behaviour.

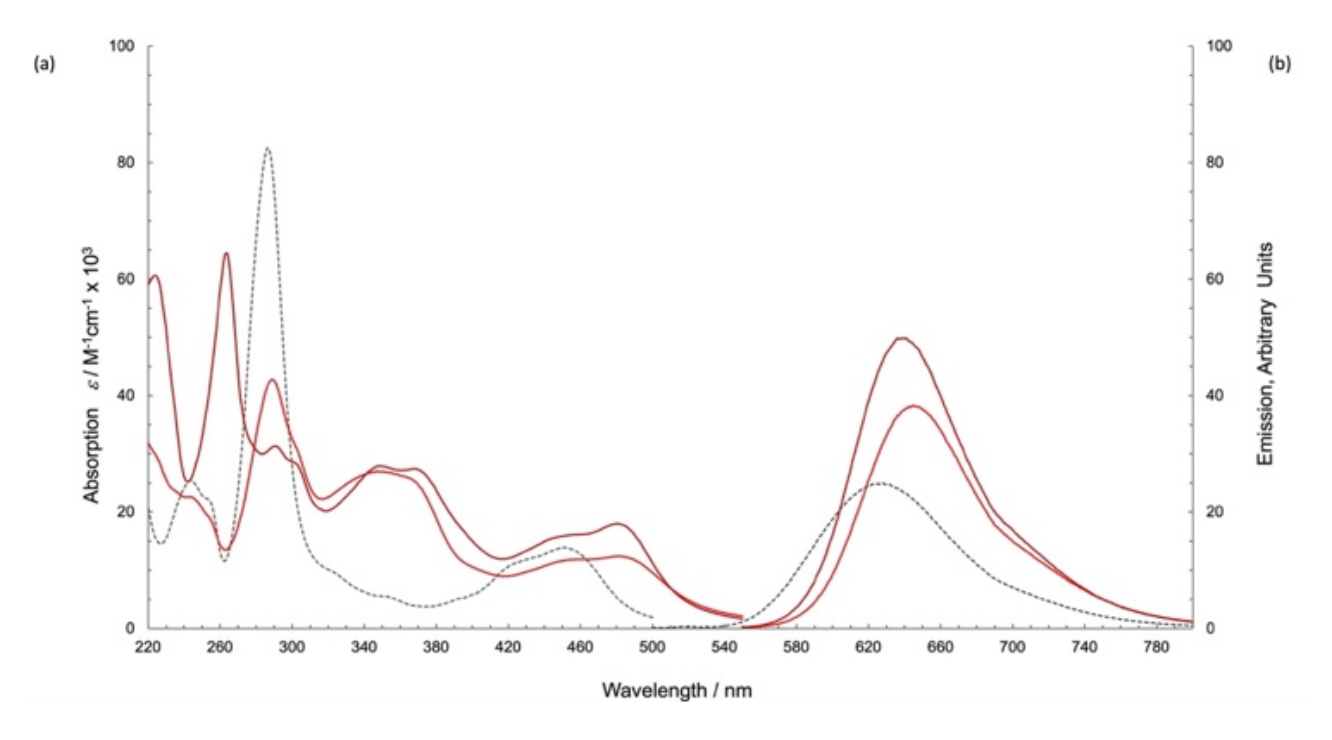


Figure 2 Photophysical characterization of $[Ru(bpy)_2(bbib)](PF_6)_2$ (red) $[Ru(phen)_2(bbib)](PF_6)_2$ (dark red) compared to $[Ru(bpy)_3](PF_6)_2$ (a) UV-Vis spectra in aerated acetonitrile at 298K and a concentration of 1 x 10⁻⁵ M; (b) the emission normalized with an absorption of 0.1 at 450 nm.

Table 1 Electronic absorption / emission data recorded at 298 K in under aerobic conditions at a concentration in the range of 1 - 5 x10⁻⁵ M.

Complex		Absorpt λmax/nm (ε/m	λr	Emission λ_{max}/nm Φ_{em}		
	LMCT	LC	LC	MLCT		
[Ru(bpy) ₂ (bbib)](PF ₆) ₂ ¹	244 (22400)	290 (42700)	348 (27000)	481 (12400)	645 ³	0.055 5
[Ru(phen) ₂ (bbib)](PF ₆) ₂ ¹	263 (63700)	290 (31400)	349 (27900)	480 (18000)	638 ³	0.069 5
[Re(bbib)(CO)3(py)](PF ₆) ¹	222 (21900)	285 (11000)	303 (11400)	363 (8650)	584 ⁴	0.041 6
trans-[lr(ppy) ₂ (bbib)](PF ₆) ²	n/a	333 (33600)	359 (31400)	480 (1830)	619 ³	0.103 5

¹ in aerated CH₃CN at 298 K

The UV/Vis absorbance and emission spectra of $[Ru(bpy)_2(bbib)]^{2+}$ and $[Ru(phen)_2(bbib)]^{2+}$ were recorded over a pH range from 2 to 12 using a standardized aqueous 0.1 M Britton-Robinson buffer and adjusted by the addition of a 0.1 M NaOH solution (Figure S11-14). The UV/Vis absorbance spectra for both complexes have several peaks which show considerable change, particularly those assumed to be associated with the bbib p to p* and the bbib MLCT transitions, with protonation of the two imidazole groups occurring in the pH range of 2 to 4. Similar changes are also seen in the emission spectra, suggesting protonation in the pH region of 4 to 5.5. The difference in the p K_a is an interesting feature, and this could relate to the differences between the p K_a of the ground and excited state. Given that the change in emission is over a broad pH range, it suggests that a sequential two-step protonation occurs and that, as pH drops, the emissive peak at 650 nm peak is quenched, and a new emissive state is observed at 720 nm consistent with a reduction in the bbib ligand LUMO energy level on protonation. There is also a noticeable change

² in aerated DMSO at 298 K.

³ excited at 450 nm

⁴ excited at 380 nm

⁵ emission quantum yield calculated relative to $[Ru(bpy)_3](PF_6)_2$ ($\Phi_{em} = 0.040$) in acetonitrile. [48]

⁶ emission quantum yields calculated relative to [Re(CO)₃Br(bpy)] (Φ_{em} = 7.8 x 10⁻³) in acetonitrile. [49]

in the absorption spectrum corresponding to deprotonation in the pH range of 9.5 to 11 and a significant blue shift in luminescence, with the emissive state switching from the bbib ³MLCT to the ancillary bpy / phen ³MLCT excited state. In these studies, given the necessity to control the pH with both hydroxide and the cocktail of acetate, borates and phosphates in the Britton-Robinson buffer, the presence of these anions might not be innocent in the observed behaviour.

Unfortunately, the complex [Re(bbib)(CO)₃(Br)] is too insoluble to complete a spectroscopic study. However the UV / vis absorption of the complex [Re(bbib)(CO)₃(py)](PF₆) was readily recorded in acetonitrile, showing that it is similarly red shifted in comparison to the parent complex [Re(bpy)(CO)₃(py)](PF₆) (MLCT λ_{max} = 366 nm, em λ_{max} = 558 nm),^[50] with a very long "tail" in the absorption stretching out to 440 nm (Figure S9). The emission is red shifted by 26 nm relative to the unfunctionalized parent complex consistent with the extended conjugation in the bbib ligand and the complex is surprisingly emissive, being comparable to the ruthenium complexes discussed above. The iridium complex [Ir(ppy)₂(bbib)](PF₆) proved to be remarkably insoluble in acetonitrile unfortunately, but in DMSO the complex could be readily dissolved, illustrating absorptions typical for this cyclometalated system (Figure S10), again with the absorption and emission redshifted in comparison to [Ir(ppy)₂(bpy)](PF₆).^[51] Due to the poor solubility of these species in aqueous solution, it was not feasible to undertake a review of the pH behaviour.

Anion Binding Studies using UV / Visible Spectroscopy

The introduction of a range of anions as the tetrabutylammonium (TBA) salts to $[Ru(bpy)_2(bbib)](PF_6)_2$, $[Ru(phen)_2(bbib)](PF_6)_2$ and $[Re(bbib)(CO)_3(py)](PF_6)$ in acetonitrile resulted in anion selective photophysical perturbations in the UV / vis. absorption spectra. (The poor solubility of $[Ir(ppy)_2(bbib)](PF_6)$ prevented inclusion in this study.) The behaviour is invariant to the addition of up to ten equivalents of CI^- , Br^- , NO_3^- , HSO_4^- and even AcO^- (Figure S15 - 17), but the addition of $H_2PO_4^-$ results in a significant and systematic change in the absorption spectra, demonstrated by a decrease in intensity in the bpy $p-p^*$ absorption, and a "flattening" of the bands attributed bbib ligand (Figure 3i) and an associated redshift, being more pronounced with the more conjugated phenanthroline co–ligands.

Similarly, the emissive behaviour of the two ruthenium complexes is invariant to the presence of Cl^- , Br^- , NO_3^- , ClO_4^- , and AcO^- (Figure 4). With the rhenium complex however, there is a stoichiometric quenching with AcO^- , and a slight increase in the emission with both Cl^- and Br^- anions which is assumed to arise from an interaction between these three anions and the available coordination site on the metal cation, rather than association with the bbib function itself. The behaviour with $H_2PO_4^-$ results in a considerable quenching of all three metal complexes (Figure 3ii) in what appears to be a multi–step process giving rise to interesting binding isotherms (inset Figure 3) with a variation in the observed behaviour choregraphed by both the metal centre and the ancillary ligands.

Given the strong interactions of these complexes with hydrogenphosphate in acetonitrile, it is possible that these persist in an aqueous environment. However, in protic solvent systems (water and MeOH), there are significant issues with precipitation as H₂PO₄ concentration increases, suggestive of a strong ion pairing between the hydrophobic cations and the anions. To maintain solubility of the neutral ion pair, the studies were undertaken in both DMSO, and DMSO containing 10% water, thereby introducing a more competitive binding environment for both the anion and the host, and increasing the hydration enthalpy that needs to be overcome. [22] These two solvent combinations permitted analysis with the less soluble iridium complex trans-[Ir(ppy)₂(bbib)](PF₆). As anticipated, the absorption and emission spectra are invariant with the addition of up to ten equivalents of Cl⁻, Br⁻, NO₃⁻, ClO₄⁻ and HSO₄⁻ for all four metal complexes, with the exception of [Ru(phen)₂(bbib)](PF₆)₂ where a slight increase in the emission is noted with HSO₄⁻ (Figure S18 – S25). The addition of AcO⁻, resulted in a significant drop in the emission ([Ru(bpy)₂(bbib)](PF₆)₂ \sim 25%, [Ru(phen)₂(bbib)](PF₆)₂ \sim 30% and [Re(CO)₃(bbib)(py)](PF₆) \sim 75%) in DMSO (Figure 5), and to a lesser extent in aquated DMSO (Figure S26). The emission from [lr(ppy)₂(bbib)](PF₆) is observed to guench with AcO (~25%), but the titration indicated an unusual "sigmoidal titration" curve, suggestive of a more complex set of equilibria associated with the binding of acetate in this one particular case (Figure 5d).

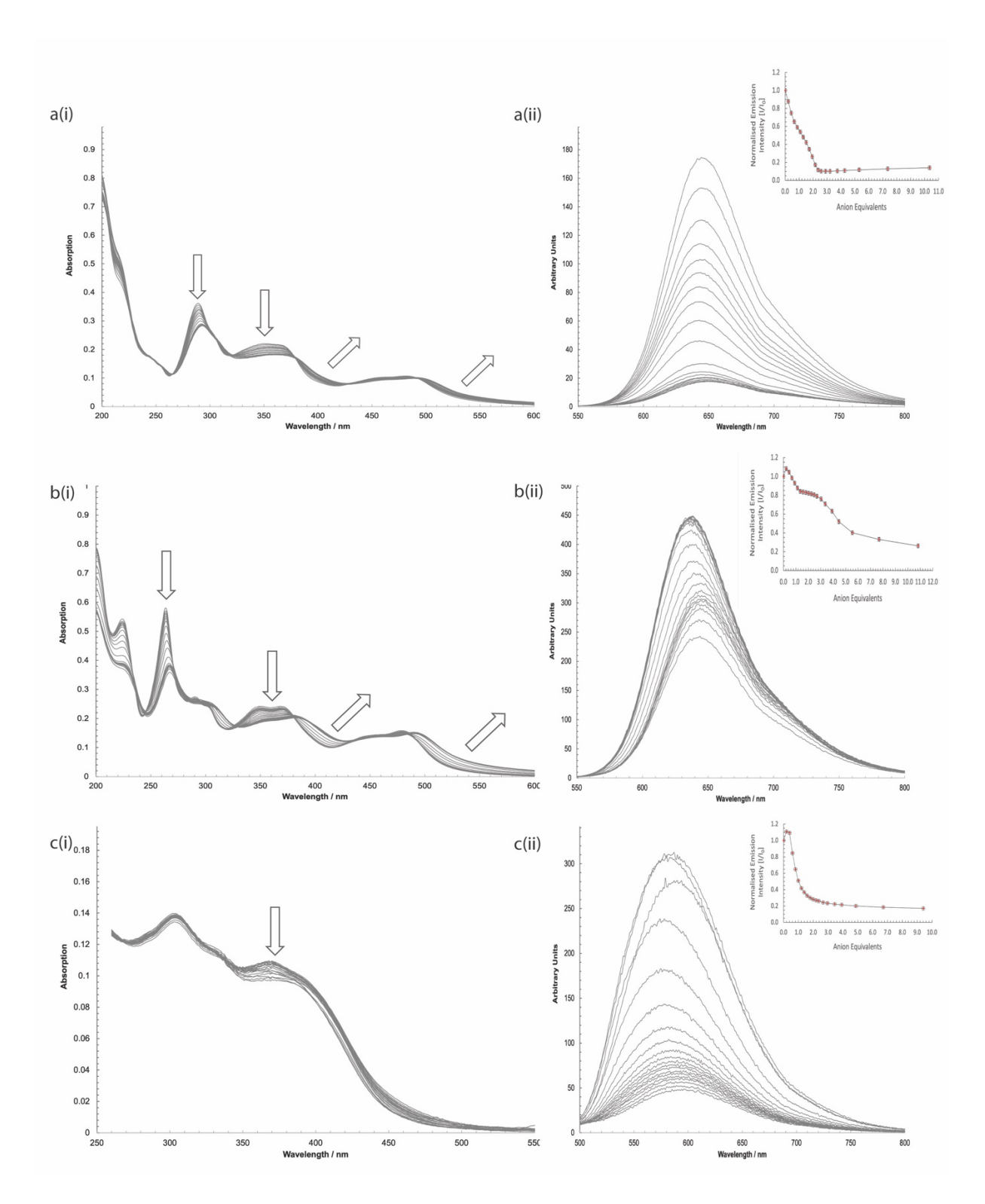


Figure 3 (i) The UV / Vis absorption spectra and (ii) emission spectra excited at 450 nm (a & b), or 380 nm (c) at 298 K in aerated acetonitrile showing the sequential addition of TBA dihydrogenphosphate (up to 10 equivalents) to (a) $[Ru(bpy)_2(bbib)](PF_6)_2$ (9.19 μ M), (b) $[Ru(phen)_2(bbib)](PF_6)_2$ (8.80 μ M) and (c) $[Re(CO)_3(bbib)(py)](PF_6)_2$ (14 μ M).

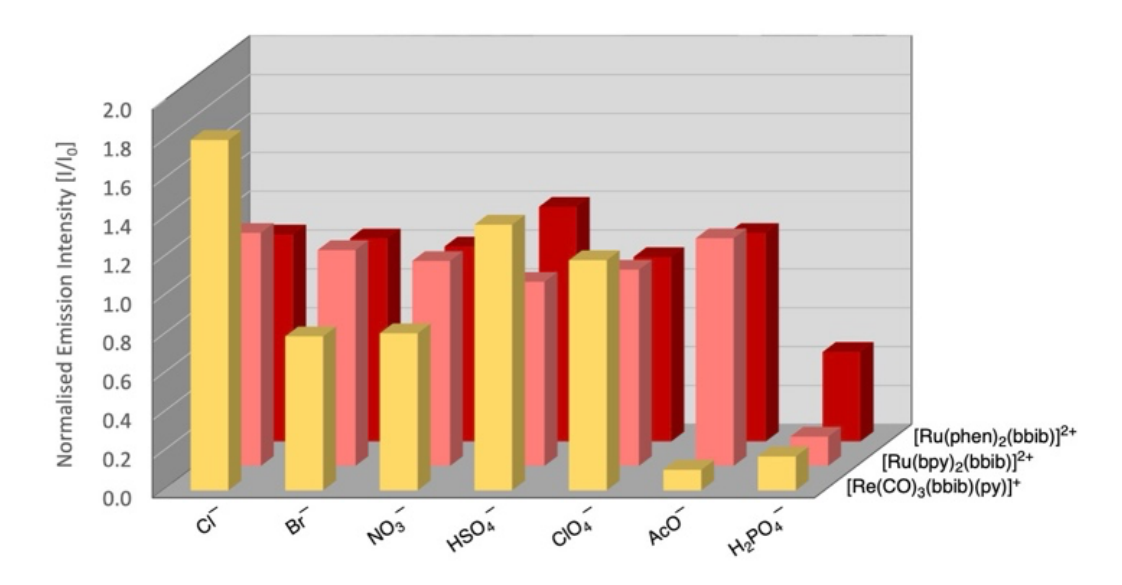


Figure 4 The change in emissive behaviour of $[Ru(bpy)_2(bbib)]^{2+}$ (red) $[Ru(phen)_2(bbib)]^{2+}$ (pink) and $[Re(CO)_3(bbib)(py)]^{2+}$ (orange) on the addition of 5 equivalents of a range of anions as TBA salts (CH₃CN, 298 K, at ~1 x 10⁻⁵ mol dm³).

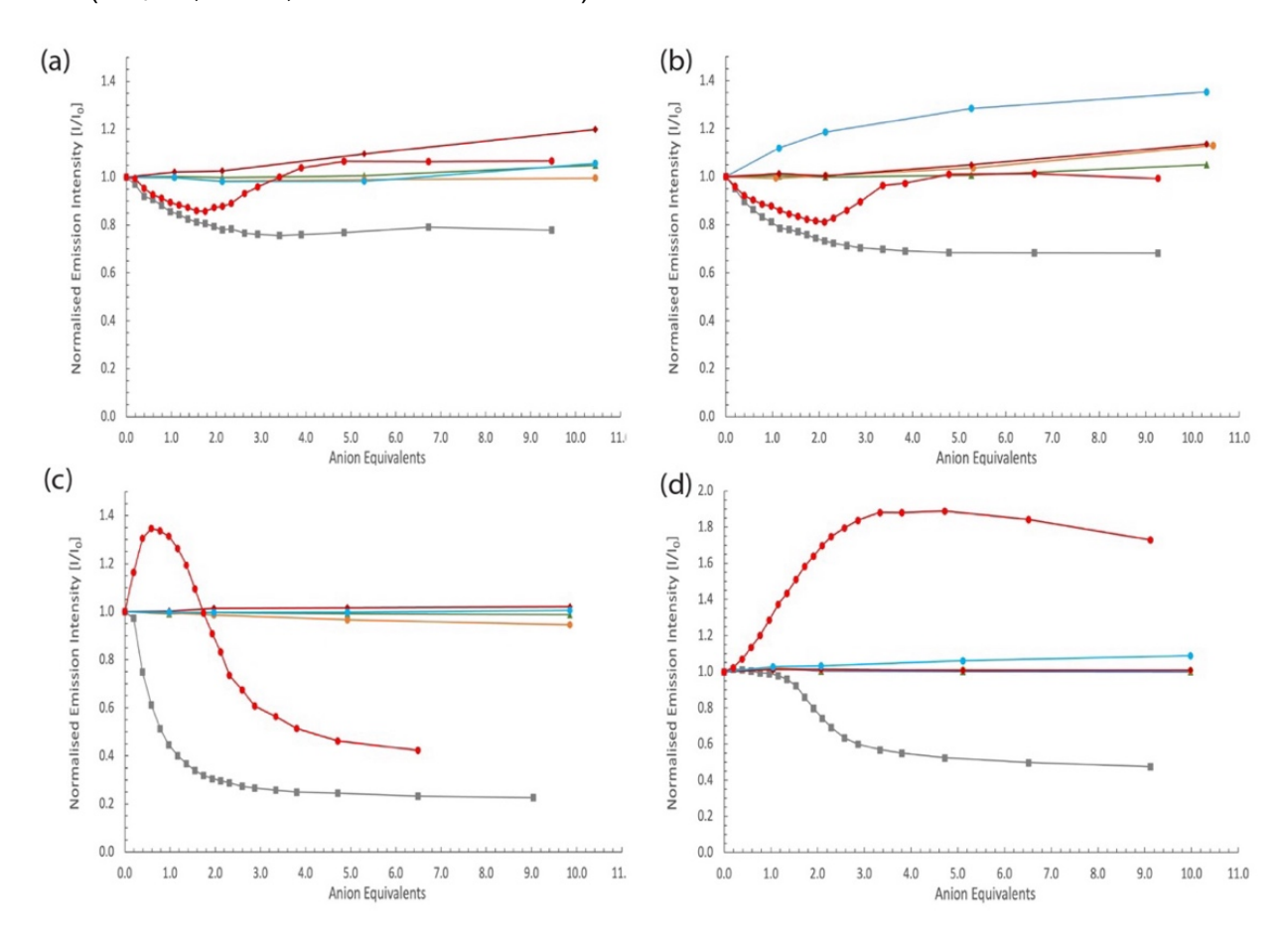


Figure 5 The change in emissive behaviour of (a) $[Ru(bpy)_2(bbib)](PF_6)_2$, (b) $[Ru(phen)_2(bbib)](PF_6)_2$, (c) $[Re(CO)_3(bbib)(py)](PF_6)_2$ and (d) $[Ir(ppy)_2(bbib)](PF_6)$ on the addition of TBA chloride (green), bromide (orange), acetate (dark blue), nitrate (purple), hydrogensulfate (pale blue) and dihydrogenphosphate (red) (DMSO) the addition of TBA chloride (green), bromide (orange), acetate (dark blue), nitrate (purple), hydrogensulfate (pale blue) and dihydrogenphosphate (red).

The addition of H₂PO₄⁻ to all four complexes in DMSO demonstrate disparate behaviour, with the absorption spectra showing considerable perturbations, as seen in acetonitrile. With the two ruthenium complexes, [Ru(bpy)₂(bbib)](PF₆)₂ and [Ru(phen)₂(bbib)](PF₆)₂, initially a quenching in the emission is seen with up to two equivalents, followed by a subsequent increase in the emission and a commensurate blue shift (660 to 654 nm and 656 to 642 nm respectively). This indicates that the interaction with this anion appears to influence both the ground and excited states of the ruthenium ³MLCT, signifying a change is imposed on the bbib ligand, but not to the extent that the complex becomes protonated. The addition of H₂PO₄⁻ to [Re(CO)₃(bbib)(py)](PF₆) similarly results in a perturbation of the absorption spectra, with an enhancement of the MLCT absorption at 340-380 nm. But contrary to the studies with the ruthenium(II) complexes, there is also an initial increase in the emission with the addition of approximately one equivalent, before significant quenching occurs (Figure 5c). Again, this is indicative of at least two different process being involved in the complex's interaction with this anion. The behaviour of [Ir(ppy)₂(bbib)](PF₆), using a more concentrated sample (approx. 6.7 x 10⁻⁴ M), with H₂PO₄⁻ (Figure 5d) interestingly results in an increase in the emission intensity, a distinctly sigmoidal association curve, and a commensurate blueshift in the emission (630 to 610 nm), as seen with the ruthenium complexes.

As anticipated, the inclusion of H_2O to the solvent system significantly decreases the measured change in absorption and emission spectra λ_{max} in comparison to those observed in DMSO (Figure S26) with only small perturbations noted in the emission spectra on the addition of AcO $^-$. Interestingly though, the response to HSO_4^- is enhanced in general, displaying behaviour more akin to that of $H_2PO_4^-$, including the significant blueshift in the emission of the associated complexes.

Anion Binding Studies using NMR spectroscopy

To establish the stoichiomentry, ¹H NMR Job plot analysis^[52] was undertaken in a 50% acetonitrile / DMSO mixture with these four complexes demonstrating the proposed one-to-one stoichiomentry with TBA AcO⁻ (Figure S27). However, the results with H₂PO₄⁻ are far from ideal (Figure S28), with no clear maximum, suggestive that that there are several different species present in equilibria. This is further hampered by considerable precipitation over a mole fraction of 0.7, given the presence of the large excess of the anion despite the inclusion of DMSO.

To further elucidate the binding behaviour of the four identified complexes $^1\text{H}-\text{NMR}$ titration studies were completed. The addition of a number of TBA salts, particularly with H_2PO_4^- in CD_3CN , and even $(\text{CD}_3)_2\text{SO}$, at concentrations appropriate for NMR spectroscopy, results in effectively a stoichiometric precipitation. More success was achieved under the conditions used in the emissive studies discussed above, namely 10% D₂O in DMSO-D₆. The complexes were each investigated by the sequential addition of the TBA salts of Cl^- , Br^- , NO_3^- , AcO^- , HSO_4^- , ClO_4^- , and H_2PO_4^- in 10% D₂O / D₆-DMSO, at a concentration between 1 and 5 mM, and perturbations to assigned signals reviewed. As anticipated the preliminary studies against Cl^- , Br^- , ClO_4^- and NO_3^- show no significant interaction with the ruthenium(II) or iridium(III) complexes, while a small interaction was observed for Cl^- and Br^- with the rhenium complex $[\text{Re}(\text{CO})_3(\text{bbib})(\text{py})](\text{PF}_6)$ consistent with the anion interacting at the "pyridine" site rather than with the bbib moiety (Figure S29-32).

For the complexes $[Ru(bpy)_2(bbib)](PF_6)_2$, and $[Ru(phen)_2(bbib)](PF_6)_2$, a number of peaks are observed to change position upon the addition of AcO^- , HSO_4^- and $H_2PO_4^-$. Due to the presence of D_2O , the NH peaks in the region of 12 to 15 ppm are absent, however, the peak at 9.49 ppm and 9.53 ppm respectively, assigned as the bbib- H^3 signal adjacent to the imidazole function, is noted to move downfield with two equivalents of $H_2PO_4^-$ to 9.90 and 9.94 ppm respectively (Figure 6). Similarly, the bbib- H^5 signal, on the other side of the imidazole group at 8.12 and 8.05 ppm experiences a similar downfield perturbation, whilst the aromatic imidazole sees a significant upfield shift, and are noted to resolve significantly. This suggests that upon interaction with phosphate, a relatively slow rotation around the bpy-imidazole bond is being slowed. It is also noted that none of the peaks associated with the bipyridine or phenanthroline co-ligands are affected by the presence of anions. A similar result is observed with AcO^- , and to a lesser extent with HSO_4^- (Figure S29 & 30).

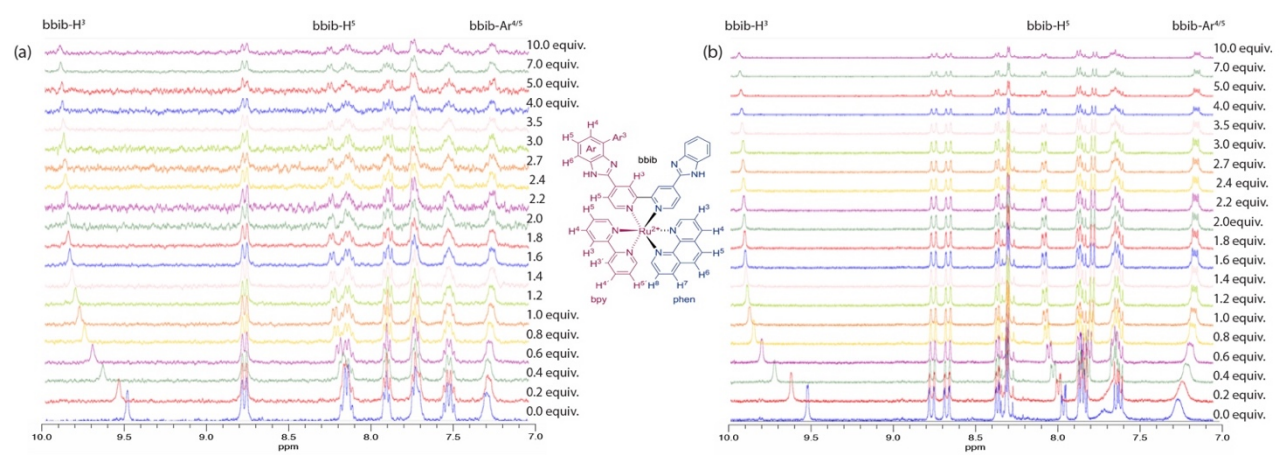


Figure 6 $^{1}\text{H-NMR}$ titration of (a) $[\text{Ru}(\text{bpy})_{2}(\text{bbib})](\text{PF}_{6})_{2}$ and (b) $[\text{Ru}(\text{phen})_{2}(\text{bbib})](\text{PF}_{6})_{2}$ and TBA $\text{H}_{2}\text{PO}_{4}^{-}$ up to ten equivalents, $\text{D}_{6}\text{-DMSO}$ + 10% D_{2}O , 298 K.

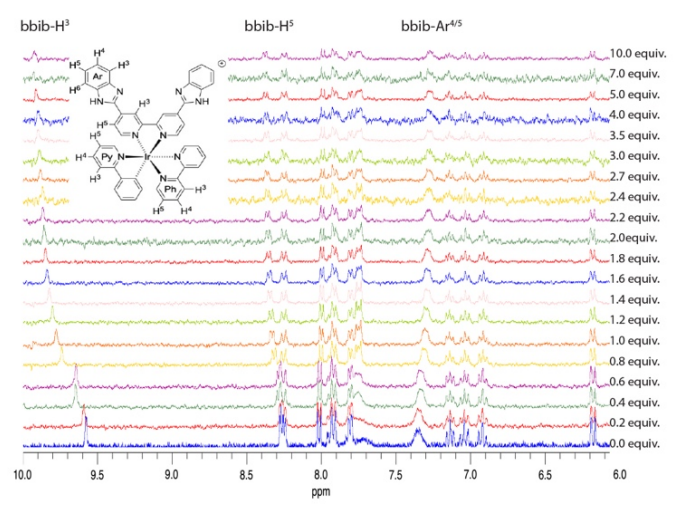


Figure 7 1 H-NMR titration of [Ir(ppy)₂(bbib)]PF₆ and TBA H₂PO₄ $^{-}$ up to ten equivalents, D₆-DMSO + 10% D₂O, 298 K.]

Table 2. Anion-Binding stability constants in 10% D₂O in DMSO-D₆

Complex	AcO [—]		$H_2PO_4^{-1}$		$H_2PO_4^{-2}$	
	p <i>K</i> _{1A}	р $oldsymbol{eta}$ 2А	p <i>K</i> _{1P}	р $oldsymbol{eta}_{2 extsf{P}}$	<i>pK</i> _{1P}	$ hoeta_2$ c
[Ru(bpy) ₂ (bbib)](PF ₆) ₂	3.42 ± 0.5	5.52 ± 0.6	4.10 ± 0.6	5.31 ± 3.2	3.81 ± 0.1	3.45 ± 0.5
[Ru(phen) ₂ (bbib)](PF ₆) ₂	3.70 ± 0.3	5.01 ± 0.7	5.23 ± 1.5	6.92 ± 3.1	n/a	n/a
[Re(bbib)(CO) ₃ (py)](PF ₆)	3.61 ± 0.5	4.82 ± 0.6	4.56 ± 3.4 ³	5.54 ± 4.13^3	n/a	n/a
trans-[Ir(ppy) ₂ (bbib)](PF ₆)	3.28 ± 0.4	6.49 ± 0.9	4.38 ± 0.4	7.26 ± 0.54	3.33 ± 0.1	5.54 ± 0.8

¹ calculated by following ¹H-NMR shift of bbib-H³ C-H proton, determined using WINEQNMR stability constant software, ^[53] using a 1:2 binding model.

Due to the fluctional nature of the complex [Re(CO)₃(bbib)(py)](PF₆), and the broadness of the benzimidazole signals, as well as the lability of the pyridine group in DMSO, which is assumed to dissociate, the 1 H NMR titrations proved difficult to interpret. However, with the addition of H₂PO₄ $^{-}$, there is an obvious change in position of the bbib-H³ proton position, presenting a sigmoidal

² calculated by following ³¹P-NMR shift of the phosphate, determined using WINEQNMR stability constant software, ^[53] using 2:1 binding model.

³ data proved difficult to obtain, based on broadening of the peaks and the model proving to be relatively unstable.

binding isotherm with increasing anion concentration, indicative of hydrogen-bond formation. The peak is shifted downfield by 0.18 ppm, and the other bbib peaks are similarly affected. The broad benzimidazole HAr proton peaks at 7.40 and 7.80 ppm are also noted to sharpen significantly and resolve into separate peaks, suggesting an induced restricted rotation of the benzimidazole moiety. A similar, but smaller interaction is observed with AcO⁻ and HSO₄⁻.

With $[Ir(ppy)_2(bbib)](PF_6)$, the bbib-H³ signal also undergoes a sigmoidal binding curve with a shift of 9.56 to 9.89 ppm (Figure 7), reminiscent of the previously reported cooperative binding to $H_2PO_4^{-}$, [26] and consistent with the UV / vis absorption studies. As with the ruthenium complexes, the peaks at 7.36 and 7.71 ppm, belonging to benzimidazole aromatic protons become sharper and resolve. Again the addition of HSO_4^{-} and AcO^{-} show similar results.

Stability constants were calculated using WINEQNMR^[53] fitting well for a one-to-two complex to anion ratio (Table 2). With all of the complexes, the interaction with AcO⁻ follows the anticipated pattern with an initial binding constant for all complexes in the order of p K_{1A} ~ 3.5, and p β_{2A} ~ 5.0 indicating two independent anions can bind to the complex in two potentially different domains (where p β_{2A} = p K_{1A} + p K_{2A} : Scheme 2). The binding of H₂PO₄⁻ on the other hand is significantly stronger than initially anticipated, with the first binding interaction being of the order of p β_{1P} ~ 4.5, approximately ten times stronger than seen with acetate. The subsequent binding of a second H₂PO₄⁻ generally is much weaker to the point that a one-to-one binding model can be readily applied. For the more hydrophobic complexes [Ru(phen)₂(bbib)](PF₆)₂ and [Ir(ppy)₂(bbib)](PF₆), p β_{2P} is larger than for [Ru(bpy)₂(bbib)](PF₆)₂ and [Re(CO)₃(bbib)(py)](PF₆) suggesting that the association of the second anion is affected by the co-ligand. With HSO₄⁻ the size of the shifts observed in the ¹H NMR titration are considerably smaller than for either AcO⁻ and H₂PO₄⁻ (and for the [Re(CO)₃(bbib)(py)](PF₆) broader), and whilst stability constants could be obtained of a similar order of magnitude to H₂PO₄⁻, the uncertainty levels were too high to have confidence in them.

Rather than following the 1 H NMR spectrum and the interaction of the host with the anion, phosphate offers a unique opportunity to follow the interaction of the anion with the host using 31 P NMR spectroscopy. The sequential addition of both [Ru(bpy)₂(bbib)](PF₆)₂ and [Ir(ppy)₂(bbib)]PF₆ to a sample of TBA salt, again in a 10% D₂O / DMSO mixture, results in detectable perturbation of the single phosphate resonance with a downfield shift from -1.48 ppm to 0.68 ppm with ten equivalents of [Ru(bpy)₂(bbib)](PF₆)₂ and to 0.59 ppm with [Ir(ppy)₂(bbib)]NO₃ (Figure 8). For both these systems stability constants were determined using WINEQNMR^[53] fitting well for a one-to-two binding model (*i.e.* one anion interacting with two complex cations), with p K_{1P} = 3.81 and p β_{2C} = 3.45 for [Ru(bpy)₂(bbib)](PF₆)₂ and p K_{1P} = 3.33 and p β_{2C} = 5.54 for [Ir(ppy)₂(bbib)](PF₆). (Scheme 3). This implies that in addition to the simplistic idea of one, and then two anions pairing with the cationic host as suggested by the initial 1 H NMR titration studies (where the anions are taken to excess), there is a third possible interaction where one anion is bound to two of the bbib functions in the presence of a high metal complex concentration, making the interaction with this tetrahedral acidic anion more complex than anticipated.

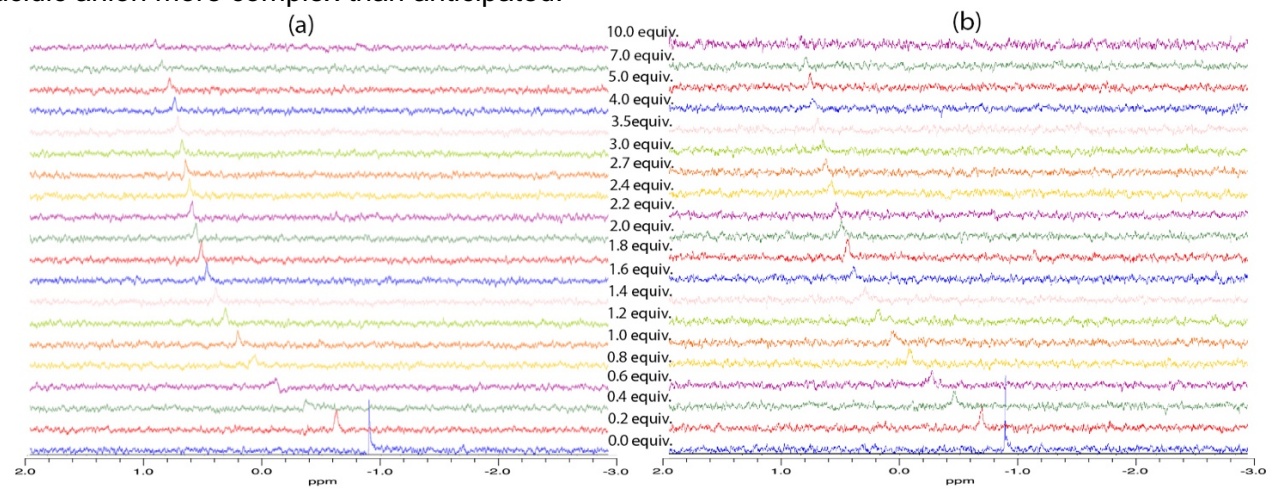


Figure 8 ^{31}P -NMR titration of $H_2PO_4^-$ and (a) [Ru(bpy)₂(bbib)](PF₆)₂ and (b) [Ir(ppy)₂(bbib)](PF₆) with up to ten equivalents, D_6 -DMSO + 10% D_2O , 298K.

X-ray Structural Analysis

Crystals of [Ru(bpy)₂(bbib)](PF₆)(H₂PO₄) were grown from an acetonitrile / methanol mixture of [Ru(bpy)₂(bbib)](PF₆)₂ and an excess of TBA H₂PO₄. In the structure of [Ru(bpy)₂(bbib)](PF₆)₂, the hexafluorophosphate anions were not associated with the metal complex (Figure 1), and whilst the packing indicated evidence of p-stacking interactions, the pair of enantiomers in the unit cell do not present any evidence of an association that would persist in solution. Contrary to this, dihydrogenphosphate locates within the "cleft" of the bbib moiety (Figure 9), with a short distance from the imidazole N and the phosphate O of 2.679 and 2.751 Å indicating a hydrogen bond interaction between the anion and the cation. Further, the separation from the phosphate oxygens to the two protons at position 3 of the bbib bipyridine is also observed to be in the range of 2.280 and 3.447 Å consistent with the observed interaction in the ¹H NMR titration studies. Whilst this structure is suggestive of a one-to-one coupling, the dihydrogenphosphate moiety then forms a hydrogen bonded dimer, linking to the other enantiomer of the ruthenium complex, resulting in a single unit consisting of two complex cations, and two linked phosphate units.

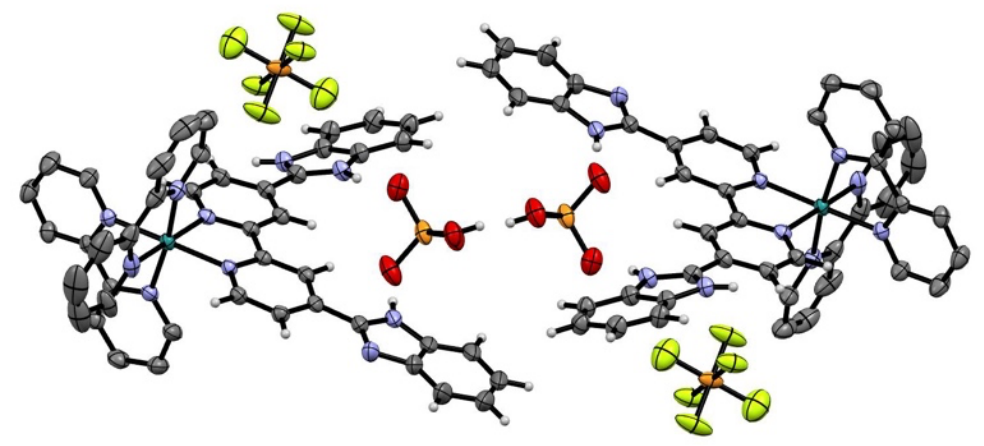


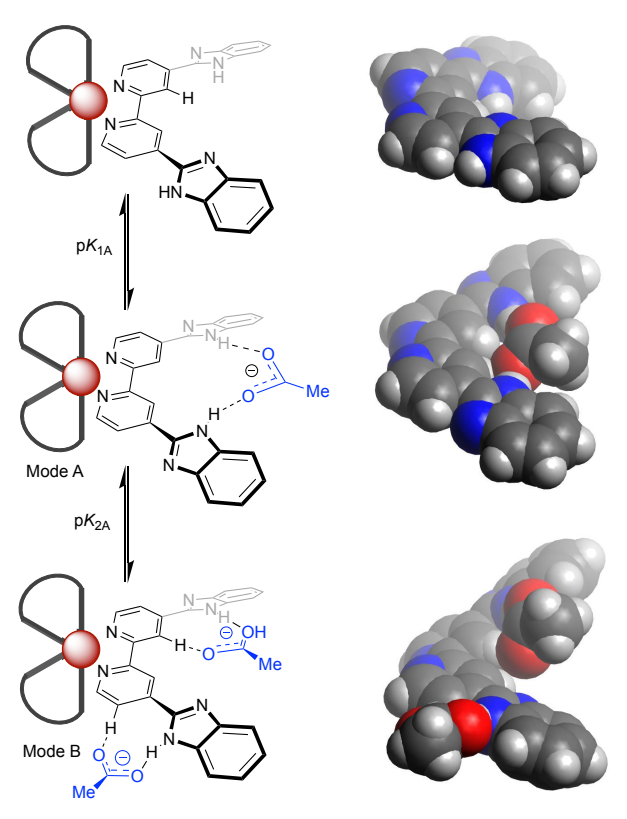
Figure 9 The X-ray structure of {[Ru(bpy)₂(bbib)](PF₆)(H₂PO₄)}₂, units with ellipsoids at 50% probability and bipyridine hydrogens omitted for clarity.

Discussion of Binding Modes and Molecular Modelling

The complexes reported here with bbib do not have an observed interaction with many of the anions investigated in this study. That does not suggest that they have no interaction with these anions, just that they do not induce a discernible perturbation in the applied spectroscopic technique. To elucidate the possible binding interactions further, optimised DFT studies (B3LYP/cc-pVDZ using Gaussian 09, Revision E01)^[54] of the free bbib ligand in the absence of the metal centre were undertaken. This resulted in an effectively planar structure for the ligand (Scheme 2), and interestingly, with most of the anions considered. There are good anion NH contacts being discerned in most cases and the interaction with chloride, bromide and perchlorate salts illustrate that both a one-to-one and a two-to-one binding mode are conceivable, with the two ligands effectively retaining their planarity, and taking an orthogonal arrangement in the latter case (Figure S33).

There are different behaviours observed spectroscopically with the addition of AcO^- and $H_2PO_4^-$, which is reflected to a lesser extent with HSO_4^- . In the former case, the interaction appears to be relatively straightforward opting primarily for a one-to-one stoichiometry from the Job plot data. This potentially relies on a hydrogen bonding interaction with the imidazole NH group, and potentially a proton on the associated bpy group (H^3). The initial association is anticipated in the "cleft" formed between the two functional groups (mode A), and then a second weaker interaction, effectively external to the bbib ligand (mode B), given that it will be more sterically demanding, especially in the case of larger co-ligands. The proposed interactions were optimised using DFT studies in the absence of the metal centre. These suggest that binding acetate causes a considerable twisting of the ligand out of a planar configuration and does not have an optimal fit. With two anions it causes a C3-C2-C2'-C4' dihedral angel to increase to 20.1° to accommodate the anion in the absence of the metal. This would account for significant perturbation in the absorption spectra and the divergent behaviour observed in the emission spectroscopy, which was especially noticeable with the complex $[Ir(ppy)_2(bbib)](PF_6)$. The variation in the emissive behaviour with this

anion is also heavily influenced by the metal centre involved, suggesting that the orientation of the ancillary ligands, and the charge of the complex also have an influence. To our knowledge, these effects have not been explored in detail and a justification is not immediately evident, although it could arise from the degree of mixing of the metal d orbitals with the co-ligands within the HOMO manifold.

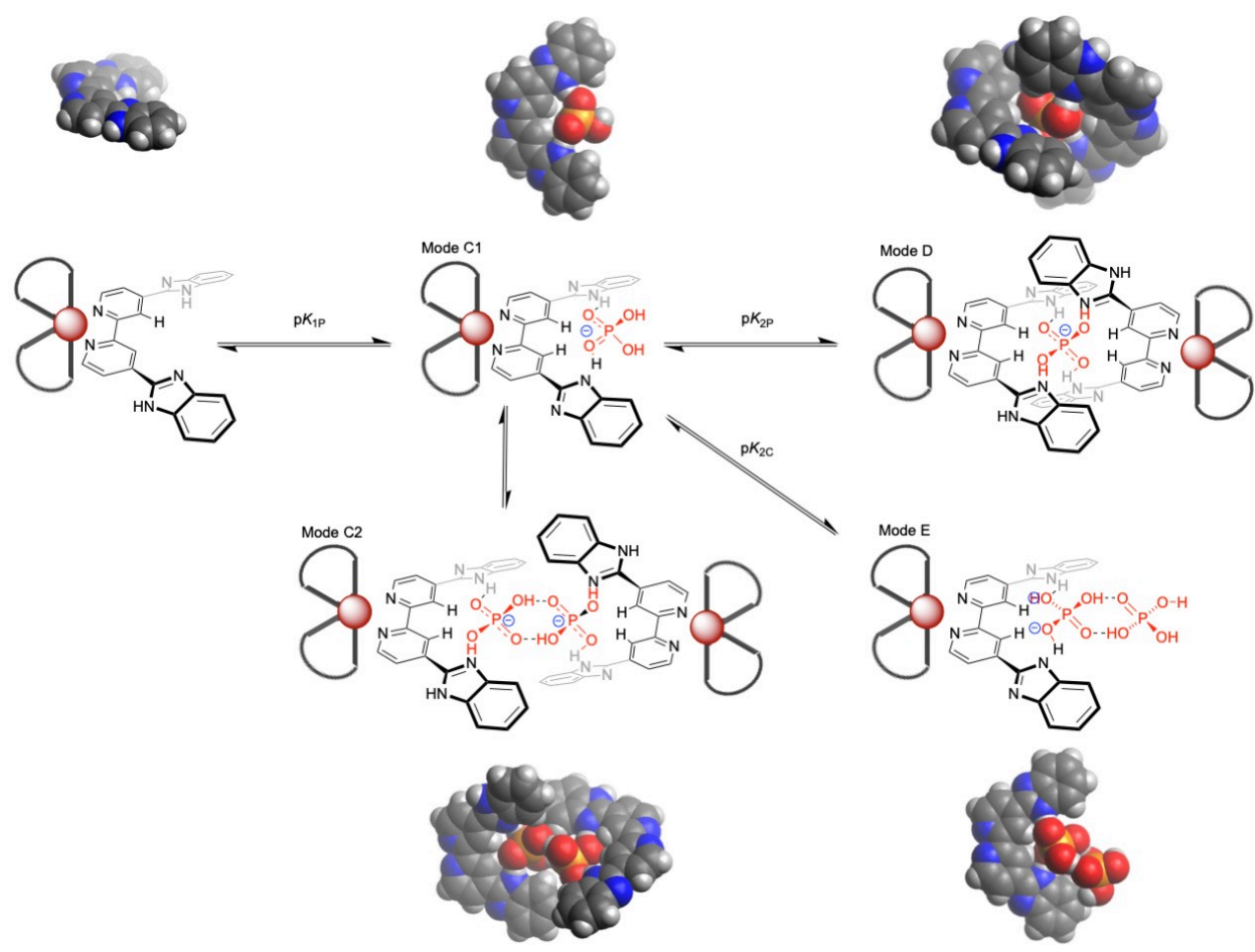


Scheme 2 Overview of the potential binding modes to the generic bbib ligand system with acetate, and associated DFT optimized structures.^[54-55]

The behaviour with $H_2PO_4^-$ differs to that of AcO⁻ with what appear to be a complex set of equilibria (Scheme 3). The NMR spectroscopic anion titrations are of the order of $pK_{1P} = 4$ for a one-to-one association which is within an order of magnitude for the data obtained for in both the ^{31}P and ^{1}H NMR determinations in 10% D_2O in DMSO. The ^{31}P NMR data suggests initially that one anion interacts with the complex (mode C1), but a further association can then occur at high complex concentration, forming a hydrogen-bonded mono-phosphate bridged dimer {[complex]}_2-H_2PO_4} (pb_{2C} ; mode D). The formation of this "dimeric form" will be significantly affected by both the steric demands and the charge on the metal complex. Conversely, if the anion is in high concentration, then a second $H_2PO_4^-$ interacts with the first, to form a phosphate dimer {[complex]}_{(H_2PO_4)_2}} (pb_{2P} ; mode E), presumably via a proton exchange between phosphates. Interestingly, the X-ray structural determination of the one-to-one adduct appears as a complex dimer (mode C2), adding a further complication to the binding equilibria.

The imidazole group is not innocent in the binding of dihydrogenphosphate, depending on whether the NH groups are pointing inwards to the "cleft", or outwards thereby facilitating proton transfer in the system, given that $H_2PO_4^-$ can also potentially act as both H-bond donor and acceptor. The pH behaviour discussed above, indicates that in the pH range involved in these studies, one would not expect that the imidazole is formally protonated, as potentially supported by the only moderate blueshift in the emission on binding the anion. To confirm this, a series of DFT studies on the free ligand were considered by both placing the imidazole proton in the external position, and moving the phosphate protons from the OH, and protonating the free imidazole proton (*i.e.* { H_2 bbib²⁺- PO_4^{3-} }, { $Hbbib^+-HPO_4^{2-}$ } and { $bbib-H_2PO_4^{-}$ }). Following optimization, the proton is transferred back to the phosphate oxygen atom, although interestingly, there is a 37.8 kcal mol⁻¹ energy difference between having the imidazole protons external, and the imidazole nitrogen acting as proton acceptor, and the more stable configuration, having them internal and acting as proton donors to

the phosphate (Figure S34). This is also noted to a lesser extent with HSO₄⁻, where the proton remains on the sulfate group, being 11.0 kcal mol⁻¹ more stable, although the bbib₂-HSO₄⁻ dimer is again the most likely species (Figure S35), and this could be responsible for what appear to be the anomalous results seen in the ¹H NMR titrations.



Scheme 3 Overview of the potential binding modes to the generic bbib ligand system with dihydrogenphosphate, and associated DFT optimized structures.^[54-55]

The additional complexity of having both hydrogen donor and acceptor groups on both the host and guest results in a delicate balance in the equilibria. The relative degree of protonation of both the anion, and the imidazole could easily give rise to considerable changes in the preferred binding modes.

The DFT studies were completed in a solvent free artificial environment though, and whilst it gives an opportunity to both rationalise and visualise the structure, it is evident that the formation of oligomeric phosphate units is influenced by the solvent which can compete for the hydrogen bonding opportunities, and this potentially explains the very variable response seen in the electronic spectra when changing between media. To draw out some generalizations, it appears that binding modes D and C2 are going to be favoured by the more hydrophobic complexes in the absence of a protic solvent. Conversely mode C1 would be preferred in protic media. The identification of dimeric binding modes D and C2 though could account for the very variable emissive behaviour on the introduction of a small quantity of the anion in the electronic titrations. In several cases, it was noted that the introduction of a sub-stoichiometric quantity of a "coordinating anion", led to a rapid change in emission, presumably arising from a small quantity of the "complex dimer", which is likely to be the dominant emissive species, having excluded solvent and oxygen from the second coordination sphere, reducing the standard routes to excited state quenching.

Conclusion

The ligand system bbib, whilst effectively insoluble in most media, will coordinate to emissive metals ruthenium(II), rhenium(I) and iridium(III) forming complexes which can readily interact with

acetate and dihydrogenphosphate, showing a high degree of selectivity over a range of other common anions in acetonitrile, DMSO, and even 10% aguated DMSO. Unfortunately, the complexes readily precipitated as the concentration of water was increased, suggesting that there is a degree of interaction, albeit potentially a simple ion pairing, that results in insoluble neutral species. The interaction with acetate appears to be typical of a hydrogen donor interaction, with a simple one to one host to complex pairing potentially from a direct hydrogen bond interaction with the imidazole. The interaction with dihydrogenphosphate, and potentially also with hydrogensulfate, has proved to be more complex, and whilst simple models to explore the speciation have been considered, the need to model several modes of binding becomes a considerable challenge, especially as a slight change in the protic environment can disturb the equilibria, and potentially the identity of the dominant species. There is a suggestion that the "dimerized" complexes are highly emissive, and so relative speciation is challenging. But the phosphate anions appear to have a unique interaction within "the cleft" of the bbib ligand, and rather than demonstrating a proton abstraction, as often seen with strong hydrogen bond donors, the binding ability appears to be far more nuanced with both the host and the anion acting as donor and acceptor resulting in a complex range of binding modes. In future studies we hope to explore the subtleties implied through these four simple complexes and discuss whether these species might exhibit selectivity for a range of important biological phosphates or demonstrate a new mode of DNA binding. Further, changes in the structure might also eliminate the interactions with acetate and sulfate and improve the selectivity by extending the imidazole framework.

Experimental Section

Physical measurements: NMR spectra were recorded using Bruker Avance III 400 spectrometer at 298 K and referenced against solvent. Absorbance spectra were recorded using a 1 cm path length quartz cuvette on an Agilent Carey 60 UV vis spectrometer. Emission spectra were recorded using a clear quartz cuvette on a Agilent Carey Eclipse spectrophotometer; quantum yields were determined by normalization against [Ru(bpy)₃]²⁺ in aerated water (Q = 0.040) and acetonitrile (0.0018)^[48] or [Re(CO)₃(Bpy)Br] in acetonitrile (0.0078).^[49] E.S.I. mass spectroscopy was recorded using a Shimadzu LCMS-IT-TOF mass spectrometer at 298K.

Materials: All reagents were purchased from either Merck or Fisher Scientific and used as supplied unless otherwise stated. Deuterated NMR solvents were acquired from Fluorochem. $[Ru(bpy)_2Cl_2]$, [56] $[Ru(phen)_2Cl_2]$ and $[\{Ir(ppy)_2(m-Cl)\}_2]^{[38a, 58]}$ were prepared by a standard literature procedures. 4,4′-Dicarboxylic acid-2,2′-bipyridine was prepared by CrO_3 oxidation of 4,4′-dimethyl-2,2′-bipyridine in 86% yield following a standard literature procedure. [59]

4,4′–**Bis(benzimidazole–2-yl)–2,2**′–**bipyridine (bbib):** 4,4′-Dicarboxylic acid–2,2′-bipyridine (2.00 g, 8.20 mmol) and o–phenylenediamine (1.77 g, 16.4 mmol) in polyphosphoric acid (5 mL) were heated to 200 °C and stirred for 24 h under a N₂ atmosphere. After cooling, the solution was slowly poured into saturated aqueous NaHCO₃ (approx. 250 mL) and stirred. The resulting brown precipitate was collected by filtration, washed with water (3 x 30 mL) and dried; Yield = 1.72 g, 2.58 mmol, 54 %. 1 H–NMR (400 MHz, d (ppm), DMSO–D₆,): 9.26 (2H, d, J = 1.7 Hz, bpyH³), 8.97 (2H, dd, J = 5.1 Hz, bpyH⁵), 8.25 (2H, dd, J = 5.13, 1.7 Hz, bpyH⁶), 7.71 (4H, m, ArH^{4/7}), 7.31 (4H, m, ArH^{5/6}). IR (cm⁻¹): 3056 (m, N–H), 2372 (w, C–H), 2111 (w, C=N), 1628 (s, C=C), 1602 (s, C=C). ESI MS (e/z) 389.15 [M + H]⁺.

[Ru(bpy)₂(bbib)](PF₆)₂: [Ru(bpy)₂Cl₂] (0.171 g, 0.35 mmol), bbib (0.141 g, 0.36 mmol) and triflic acid (0.5 mL) in ethylene glycol (30 mL) were heated to 140 °C and stirred under a N₂ atmosphere for 4 h. After cooling, the crude product was precipitated by the addition of excess saturated aqueous KPF₆ and the resulting red solid isolated by filtration, washed with water (3 x 30 mL) and dried. This was purified by LH20 Sephadex® size exclusion chromatography, eluting using a 48:48:4 methanol : acetone: triethylamine mixture, and recrystallized from acetone (2 mL) and addition of aqueous KPF₆ (~0.5 g, 100 mL) as a red crystalline solid; Yield = 0.208 g, 54 %. 1 H-NMR (400 MHz, d (ppm), acetone-D₆): 12.77 (2H, br, NH), 9.58 (2H, d, J = 1.5 Hz, bbibH³), 8.88 (4H, dd, J = 8.4, 1.2 Hz, bpyH^{3,3'}), 8.37 (2H, d, J = 6.0 Hz, bbibH⁶) 8.30-8.24 (8H, m, bbibH⁵/bpyH^{6,4,4'}), 8.11 (2H, dd, J = 5.60, 1.4 Hz, bpyH^{6'}), 7.81 (4H, m, HAr^{4,7}), 7.68-58 (4H, m,

bpyH^{5,5'}) 7.45 (4H, m, HAr^{6,5}). IR cm⁻¹: 3112 (m, N-H), 2924 (m, N-H), 2111 (w, C=N), 1617 (s, C=C), 1444 (s, C-N), 1420 (s, C-N). ESI MS (m/z) 401.0908 [M]²⁺.

[Ru(phen)₂(bbib)](PF₆)₂: Prepared according to the procedure for [Ru(bpy)₂(bbib)](PF₆)₂ using [Ru(phen)₂(Cl)₂] (0.266 g, 0.50 mmol) and bbib (0.195 g, 0.50 mmol). The crude product was purified using a LH20 Sephadex® size exclusion chromatography, eluting with 70:30 methanol to acetonitrile mixture followed by second column, eluted at 90:10 methanol to acetonitrile mixture and recrystallized from acetone (2 mL) and addition of aqueous KPF6 (~0.5 g in 100 mL) as a red crystalline solid; Yield = 0.267 g, 46 %. Yield = 266 mg, 46 %. 1 H-NMR (400 MHz, d (ppm), acetone-D₆): 12.67 (2H, b, NH) 9.67 (2H, b, bbibH³) 8.89 (2H, dd, J = 8.3, 1.3 Hz, phenH⁴), 8.80 (2H, dd, J = 8.3, 1.3 Hz, phenH⁷), 8.79 (2H, dd, J = 5.3, 1.2 Hz, bbibH⁶), 8.47 (2H, d, J = 8.9 Hz, phenH⁵), 8.43 (2H, d, J = 8.9 Hz, phenH⁶), 8.33 (2H, dd, J = 5.2, 1.2 Hz, phenH²), 8.27 (2H, d, J = 5.9 Hz, bbibH⁵), 8.15 (2H, dd, J = 6.0, 1.80 Hz, phenH⁹), 8.02 (1H, dd, J = 8.3, 5.2 Hz, phenH³), 7.80 (2H, dd, J = 8.3, 5.2 Hz, phenH⁸), 7.77 (2H, bd, J = 7.7 Hz, HAr⁴), 7.73 (2H, bd, J = 7.7 Hz, HAr⁷), 7.41 (2H, bt, J = 7.5 Hz, HAr⁵), 7.33 (2H, bt, J = 7.5 Hz, HAr⁶). IR cm⁻¹: 3420 (w, N-H), 2920 (m, N-H), 2851 (m, N-H), 2111 (w, C=N), 1700 (m, C=C), 1619 (m, C=C), 1455 (m, C-N), 1420 (m, C-N). ESI MS (m/z) 425.0910 [M]²⁺.

[Re(bbib)(CO)₃Br]: Re(CO)₅Br (0.150 g, 0.37 mmol) and bbib (0.144 g, 0.37 mmol) were ground to fine powders and added to DMSO (2 mL) and stirred at 150 °C for 24 h. The crude product was precipitated by adding water (50 mL) and captured on Celite©, washed with water (2 x 25 mL) and dried in air. The product was taken into THF (~100 mL) before evaporation to give a red/orange crystalline solid; Yield = 0.102 g, 0.14 mmol, 38 %. 1 H-NMR (400 MHz, d (ppm), acetone-D₆, in the presence of a large excess of TBABr): 13.80 (2H, s, N-H) 10.47 (2H, br, bbibH³), 9.25 (2H, d, J = 5.9, Hz, bbibH⁶), 8.64 (2H, dd, J = 5.9, 1.7 Hz, bbibH⁵), 7.83 (2H, d, J = 8.7 Hz, HAr⁴), 7.80 (2H, t, J = 8.7 Hz, HAr³), 7.42 (2H, t, J = 7.6 Hz, HAr⁶) 7.34 (2H, t, J = 7.6 Hz, HAr⁵). IR cm⁻¹: 2957 (s, N-H), 2873 (s, N-H), 2018 (m, C=N), 1892 (m, C=O), 1610 (w, C=C), 1474 (s, C-N), 1379 (m, C-N). ESI MS (m/z) 736.9907 [M-H]⁺ (in presence of excess TBABr) or 700.1058 [M-Br+CH₃CN)]⁺ in acetonitrile.

[Re(bbib)(CO)₃(Py)](PF₆): [Re(bbib)(CO)₃Br] (0.039 g, 0.053 mmol) dissolved in THF (10 mL) was added to a large excess of AgClO₄ (0.013 g, 0.063 mmol) and pyridine (5 mL) and stirred for 16 h. The mixture was filtered, and cold water (20 ml) added to the filtrate and the resulting precipitate collected as a dark yellow/orange solid. The crude product was dissolved in methanol (~10 mL) and precipitated by the addition of aqueous KPF₆ (~0.5 g mL); Yield = 0.031 g, 0.042 mmol, 81 %.¹H-NMR (400 MHz, d (ppm), 90% DMSO-D₆ – 10% D₂O): 13.96 (2H, s, N-H), 9.51 (2H, d, J = 5.9, Hz, bbibH⁶), 9.41 (2H, bs, bbibH3), 8.56 (4H, m, pyH2/3, bbibH⁵), 7.87 (1H, m, pyH⁴), 7.85 – 7.72 (4H, b, HAr^{4/7}), 7.47 (2H, t, J = 7.0 Hz, pyH^{3/5}), 7.40 (4H, b, HAr^{6/5}). IR cm⁻¹: 3630 (m, N-H), 2953 (m, N-H), 2918 (m, N-H), 2868 (m, N-H), 2029 (s, C=N), 1912 (s, C-H), 1617 (s, C=C), 1420 (s, C-N). ESI MS (m/z) 738.1232 [M-PF₆]⁺.

trans–[Ir(ppy)₂(bbib)](PF₆): [{Ir(ppy)₂(m−Cl)}₂] (0.181 g, 0.169 mmol) and bbib (0.135 g, 0.348 mmol) were ground to fine powders and added to minimum DMSO (2 mL) and stirred at and stirred at 150 °C for 16 h. After cooling, the crude product was precipitated by addition of H₂O (100 mL) and captured on Celite©, washed with water (3 x 30 mL) and dried in air. Following extraction into methanol (~100 mL), the crude product was purified by silica column chromatography, eluting using a 50:50 toluene: acetonitrile solvent mixture saturated with KNO₃. The product was obtained by slowly diluting the eluent mixture with methanol (up to 10%) and triethylamine (1 %). Collected product was dissolved in minimum acetone (2 mL) and precipitated by the addition of and addition of aqueous KPF6 (~0.5 g in 100 mL) as an orange crystalline solid; Yield = 0.053 g, 15 %. 1 H−NMR (400 MHz, d (ppm), acetone−D₆): 12.02 (2H, s, N−H), 10.70 (2H, bs, bbibH³), 8.45 (2H, dd, J = 5.8, 1.7 Hz, bbibH⁶), 8.27 (2H, d, J = 7.9 Hz, pyH³), 8.16 (2H, d, J = 5.8 Hz, bbibH⁵), 8.10 (2H, d, J = 5.8 Hz, pyH⁶), 7.97 (2H, ddd, J = 8.6, 7.4 Hz, pyH³), 7.95 (2H, d, J = 7.8 Hz, phH³), 7.77 (4H, d, J = 8.6 Hz, HAr^{4/7}), 7.41 (2H, dd, J = 8.6, 7.4 Hz, HAr⁵), 7.32 (2H, dd, J = 8.6, 7.4 Hz, HAr⁶), 7.18 (2H, ddd, J = 7.40, 5.9, 1.4 Hz, pyH⁵), 7.09 (2H, ddd, J = 7.8, 7.4, 1.3 Hz, phH⁴), 6.97 (2H, ddd, J = 7.6, 7.4, 1.4 Hz, phH⁵), 6.43 (2H, d, J = 7.5 Hz, phH⁶). IR cm⁻¹: 3052 (m, N−H), 2924

(m, N-H), 2599 (m, N-H), 2497 (m, C-H), 2111 (w, C=N), 1619 (s, C=C), 1474 (s, C-H). ESI MS (m/z) $889.2376 \, [\text{M}]^{+}$.

X-ray crystallography: Single crystals were mounted on a Mitegen loop using Paratone–N oil and were cooled under a stream of nitrogen. Figures and tables were generated using OLEX2. ^[60] Crystal data were collected on a Rigaku Oxford Diffraction SuperNova diffractometer using Cu Kα radiation; the structures were solved by direct methods using ShelXT^[61] and refined by least squares using ShelXL. ^[62]

Crystals of bbib were grown from DMSO– D_6 by slow evaporation leading to small colourless blocks. Crystal Data CCDC No 2287913: for $C_{24}H_{16}N_6 \cdot (C_2H_6OS)_2$ (M = 544.68 g/mol): triclinic, space group P–1 (no. 2), a = 4.79980(10) Å, b = 9.4816(2) Å, c = 14.1642(5) Å, α = 92.168(2)°, β = 94.662(3)°, γ = 93.809(2)°, γ = 640.45(3) ų, γ = 1, γ = 100(1) K, γ = 100(1) K, γ = 2.205 mm–1, γ = 1.412 g/cm³, 4900 reflections measured (9.356° ≤ 20 ≤ 153.396°), 4900 unique (γ = 0.0140) which were used in all calculations. The final γ = 1.412 g/cm³ and γ = 1.419 (all data) using twinned data refinement: component 2 rotated by -179.94 degrees around [-0.00 -0.00 1.00] (reciprocal) or [0.24 0.06 0.97] (direct); mass fraction scales: 0.5461(17) / 0.4539(17).

Crystals of [Ru(bpy)₂(bbib)](PF₆)₂ were grown from an acetonitrile methanol by slow evaporation as dark red small blocks. Crystal Data CCDC No 2326492: for C₄₄H₃₂F₁₂N₁₀P₂Ru (M =1091.80 g/mol): triclinic, space group P-1 (no. 2), a = 9.8624(2) Å, b = 12.2271(3) Å, c = 19.5873(6) Å, α = 82.641(2)°, β = 78.128(2)°, γ = 76.288(2)°, V = 2237.77(10) ų, Z = 2, T = 100.4(7) K, μ (Cu K α) = 4.374 mm⁻¹, D_{calc} = 1.620 g/cm³, 22226 reflections measured (7.468° ≤ 2 Θ ≤ 153.174°), 22226 unique (R_{int} = ?, R_s = 0.0277) which were used in all calculations. The final R_1 was 0.0836 (I > 2 σ (I)) and w R_2 was 0.2273 (all data).

Crystals of [Ru(bpy)₂(bbib)](PF₆)(H₂PO₄) were grown from an acetonitrile / methanol mixture of [Ru(bpy)₂(bbib)](PF₆)₂ and 2 equivalents of tetrabutylammonium dihydrogenphosphate by slow evaporation as needles. Crystal Data CCDC No 2326491: for $C_{88}H_{70}F_6N_{20}O_8P_3Ru_2$ (M =1944.69 g/mol): monoclinic, space group P21/n (no. 14), a = 15.87488(13) Å, b = 14.44581(9) Å, c = 21.80418(18) Å, β = 109.8556(9)°, V = 4703.00(7) ų, Z = 2, T = 100.01(10) K, μ (Cu K α) = 3.720 mm⁻¹, D_{calc} = 1.373 g/cm³, 49162 reflections measured (7.486° ≤ 2 Θ ≤ 152.998°), 9762 unique (R_{int} = 0.0364, R_s = 0.0249) which were used in all calculations. The final R_1 was 0.0415 (I > 2 σ (I)) and w R_2 was 0.1189 (all data).

DFT studies: All calculations were performed on the Gaussian 09 Software,^[54] using default functionals and basis sets, on the free ligand. The structures were optimized using B3LYP as a functional, which has been widely used in combination with the correlation consistent basis set cc-pVTZ. Visualisation and analysis was undertaken using Avogadro 1.2.0.^[55]

Acknowledgements

C.L.H. and A.J.S. acknowledges Ph.D. funding from Lancaster University, JNL acknowledges Ph.D. funding from Lancaster university EPSRC DTP (EP/N509504/1). This research has been supported by Lancaster University. The input from Caitriona Spillane in the initial preparation of $[Ru(bpy)_2(bbib)](PF_6)_2$ is gratefully acknowledged. [46]

Keywords: ruthenium, iridium, anion-recognition, phosphate, diimine-ligands, imidazoles.

Bibliography:

- (a) L. J. Chen, S. N. Berry, X. Wu, E. N. W. Howe, P. A. Gale, Chem 2020, 6, 61-141; (b) P. A. Gale, E. N. W. Howe, X. Wu, M. J. Spooner, Coord. Chem. Rev. 2018, 375, 333-372; (c) L. K. Macreadie, A. M. Gilchrist, D. A. McNaughton, W. G. Ryder, M. Fares, P. A. Gale, Chem 2022, 8, 46-118; (d) J. Zhao, D. Yang, X. J. Yang, B. Wu, Coord. Chem. Rev. 2019, 378, 415-444.
- [2] N. Busschaert, C. Caltagirone, W. Van Rossom, P. A. Gale, *Chem. Rev.* 2015, 115, 8038-8155.

- [3] (a) R. Hein, P. D. Beer, *Chem. Sci.* **2022**, *13*, 7098-7125; (b) J. Pancholi, P. D. Beer, *Coord. Chem. Rev.* **2020**, *416*; (c) M. S. Taylor, *Coord. Chem. Rev.* **2020**, *413*.
- [4] (a) R. Plais, G. Clavier, J. Y. Salpin, A. Gaucher, D. Prim, Eur. J. Org. Chem. 2023, 26, 19; (b) I. A. Rather, S. A. Wagay, R. Ali, Coord. Chem. Rev. 2020, 415; (c) D. X. Wang, M. X. Wang, Accounts Chem. Res. 2020, 53, 1364-1380.
- [5] (a) B. K. Billing, M. Verma, ChemistrySelect 2021, 6, 4273-4284; (b) U. Manna, G. Das, Coord. Chem. Rev. 2021, 427, 21.
- [6] S. A. Boer, E. M. Foyle, C. M. Thomas, N. G. White, Chem. Soc. Rev. 2019, 48, 2596-2614.
- (a) S. Kundu, T. K. Egboluche, M. A. Hossain, *Accounts Chem. Res.* 2023, 56, 1320-1329;
 (b) V. Kumar, *Bull. Chem. Soc. Jpn.* 2021, 94, 309-326.
- [8] M. Wenzel, J. Steup, K. Ohto, J. J. Weigand, *Chem. Lett.* **2022**, *51*, 20-29.
- [9] (a) J. D. Einkauf, V. S. Bryantsev, B. A. Moyer, R. Custelcean, *Chem. -Eur. J.* 2022, 28; (b) J. de Jong, B. Feringa, S. J. Wezenberg, *ChemPhysChem* 2019, 20, 3306-3310.
- [10] G. I. Vargas-Zuniga, J. L. Sessler, Coord. Chem. Rev. 2017, 345, 281-296.
- [11] M. Batool, Z. Afzal, I. S. Khan, A. R. Solangi, Crit. Rev. Anal. Chem. 2023, 9.
- [12] E. M. Foyle, N. G. White, Chem. -Asian. J. 2021, 16, 575-587.
- [13] Y. Hu, S. S. Long, H. Y. Fu, Y. B. She, Z. C. Xu, J. Y. Yoon, Chem. Soc. Rev. 2021, 50, 589-618.
- [14] (a) A. E. Hargrove, S. Nieto, T. Z. Zhang, J. L. Sessler, E. V. Anslyn, Chem. Rev. 2011, 111, 6603-6782; (b) A. K. H. Hirsch, F. R. Fischer, F. Diederich, Angew. Chem. Int. Edit. 2007, 46, 338-352.
- (a) M. W. Bowler, M. J. Cliff, J. P. Waltho, G. M. Blackburn, *New J. Chem.* **2010**, *34*, 784-794;
 (b) S. C. L. Kamerlin, P. K. Sharma, R. B. Prasad, A. Warshel, *Q. Rev. Biophys.* **2013**, *46*, 1-132.
- [16] (a) M. V. R. Raju, S. M. Harris, V. C. Pierre, *Chem. Soc. Rev.* 2020, 49, 1090-1108; (b) S. Pal, T. K. Ghosh, R. Ghosh, S. Mondal, P. Ghosh, *Coord. Chem. Rev.* 2020, 405; (c) J. Wongkongkatep, A. Ojida, I. Hamachi, *Top. Curr. Chem.* 2017, 375, 33; (d) S. Berchmans, T. B. Issa, P. Singh, *Anal. Chim. Acta* 2012, 729, 7-20.
- [17] S. Anbu, A. Paul, G. J. Stasiuk, A. J. L. Pombeiro, Coord. Chem. Rev. 2021, 431, 48.
- [18] S. Sivagnanam, P. Mahato, P. Das, *Org. Biomol. Chem.* **2023**, *21*, 3942-3983.
- [19] (a) W. Q. Meng, A. C. Sedgwick, N. Kwon, M. X. Sun, K. Xiao, X. P. He, E. V. Anslyn, T. D. James, J. Yoon, *Chem. Soc. Rev.* 2023, 52, 601-662; (b) B. Sen, M. Rabha, S. K. Sheet, D. Koner, N. Saha, S. Khatua, *Inorg. Chem. Front.* 2021, 8, 669-683; (c) R. Puglisi, A. Pappalardo, A. Gulino, G. T. Sfrazzetto, *ACS Omega* 2019, 4, 7550-7555; (d) N. A. Esipenko, P. Koutnik, T. Minami, L. Mosca, V. M. Lynch, G. V. Zyryanov, P. Anzenbacher, *Chem. Sci.* 2013, 4, 3617-3623.
- [20] C. G. P. Taylor, A. J. Metherell, S. P. Argent, F. M. Ashour, N. H. Williams, M. D. Ward, *Chem. Eur. J.* **2020**, *26*, 3065-3073.
- [21] Y. Marcus, Biophys. Chem. 1994, 51, 111-127.
- [22] (a) S. Kubik, Chem. Soc. Rev. 2010, 39, 3648-3663; (b) S. Kubik, Chem. Open 2022, 11, 26.
- [23] (a) C. R. Rice, C. Slater, R. A. Faulkner, R. L. Allan, *Angew. Chem. Int. Edit.* **2018**, *57*, 13071-13075; (b) S. K. Dey, G. Das, *Dalton Trans.* **2011**, *40*, 12048-12051.
- [24] W. Zhao, A. H. Flood, N. G. White, Chem. Soc. Rev. 2020, 49, 7893-7906.
- [25] (a) B. Wu, C. R. Huo, S. G. Li, Y. X. Zhao, X. J. Yang, Z. Anorg. Allg. Chem. 2015, 641, 1786-1791; (b) T. S. C. MacDonald, B. Feringa, W. S. Price, S. J. Wezenberg, J. E. Beves, J. Am. Chem. Soc. 2020, 142, 20014-20020.
- [26] A. L. Blackburn, N. A. C. Baker, N. C. Fletcher, RSC Adv. 2014, 4, 18442-18452.
- (a) A. Pal, M. Karmakar, S. R. Bhatta, A. Thakur, *Coord. Chem. Rev.* 2021, 448, 55; (b) D. A. McNaughton, M. Fares, G. Picci, P. A. Gale, C. Caltagirone, *Coord. Chem. Rev.* 2021, 427, 44; (c) P. Kumar, S. Pachisia, R. Gupta, *Inorg. Chem. Front.* 2021, 8, 3587-3607.
- [28] T. Sakamoto, A. Ojida, I. Hamachi, Chem. Commun. 2009, 141-152.
- [29] (a) S. E. Bodman, S. J. Butler, *Chem. Sci.* 2021, *12*, 2716-2734; (b) J. Sahoo, C. Krishnaraj,
 J. M. Sun, B. B. Panda, P. S. Subramanian, H. S. Jena, *Coord. Chem. Rev.* 2022, *466*, 21.
- [30] (a) S. H. Hewitt, G. Macey, R. Mailhot, M. R. J. Elsegood, F. Duarte, A. M. Kenwright, S. J. Butler, *Chem. Sci.* 2020, 11, 3619-3628; (b) S. E. Bodman, C. Breen, F. Plasser, S. J. Butler, *Org. Chem. Front.* 2022, 9, 5494-5504; (c) S. Farshbaf, K. Dey, W. Mochida, M. Kanakubo, R. Nishiyabu, Y. Kubo, P. Anzenbacher, *New J. Chem.* 2022, 46, 1839-1844.

- [31] (a) K.-C. Chang, S.-S. Sun, M. O. Odago, A. J. Lees, *Coord. Chem. Rev.* 2015, 284, 111-123;
 (b) A. Rashid, S. Mondal, P. Ghosh, *Molecules* 2023, 28, 40;
 (c) M. M. Wu, Z. X. Zhang, J. X. Yong, P. M. Schenk, D. H. Tian, Z. P. Xu, R. Zhang, *Top. Curr. Chem.* 2022, 380, 45.
- [32] N. C. Fletcher, M. C. Lagunas, Topics Organomet. Chem. 2009, 28, 143-170.
- [33] (a) A. Rashid, S. Mondal, S. Mondal, P. Ghosh, *Chem. Asian. J.* 2022, 17; (b) D. L. Ma, S. Lin, W. H. Wang, C. Yang, C. H. Leung, *Chem. Sci.* 2017, 8, 878-889; (c) A. Rashid, S. Mondal, P. Ghosh, *Inorg. Chim. Acta.* 2023, 550, 8.
- [34] A. Ramdass, V. Sathish, M. Velayudham, P. Thanasekaran, S. Rajagopal, *ChemistrySelect* **2018**, 3, 2277-2285.
- [35] S. K. Patra, M. Rabha, B. Sen, K. Aguan, S. Khatua, *Dalton Trans.* **2023**, *52*, 2592-2602.
- [36] X. F. Shang, J. W. Li, H. Lin, P. Jiang, Z. S. Cai, H. K. Lin, *Dalton Trans.* **2009**, 2096-2102.
- [37] S. Naithani, T. Goswami, F. Thetiot, S. Kumar, Coord. Chem. Rev. 2023, 475, 43.
- [38] (a) F. Gärtner, D. Cozzula, S. Losse, A. Boddien, G. Anilkumar, H. Junge, T. Schulz, N. Marquet, A. Spannenberg, S. Gladiali, M. Beller, *Chem.-Eur. J.* 2011, 17, 6998-7006; (b) S. A. Rommel, D. Sorsche, M. Fleischmann, S. Rau, *Chem. Eur. J.* 2017, 23, 18101-18119; (c) S. A. Rommel, D. Sorsche, A. Dixit, S. Rau, *Eur. J. Inorg. Chem.* 2016, 40-48; (d) S. A. Rommel, D. Sorsche, S. Rau, *Dalton Trans.* 2016, 45, 74-77; (e) D. Sorsche, S. Rau, *Eur. J. Inorg. Chem.* 2014, 4244-4249; (f) H. J. Mo, H. Y. Chao, B. H. Ye, *Inorg. Chem. Commun.* 2013, 35, 100-103; (g) H. J. Mo, Y. L. Niu, M. Zhang, Z. P. Qiao, B. H. Ye, *Dalton Trans.* 2011, 40, 8218-8225; (h) Y. Cui, Y. L. Niu, M. L. Cao, K. Wang, H. J. Mo, Y. R. Zhong, B. H. Ye, *Inorg. Chem.* 2008, 47, 5616-5624; (i) J. C. Freys, G. Bernardinelli, O. S. Wenger, *Chem. Commun.* 2008, 4267-4269; (j) Y. Cui, H. J. Mo, J. C. Chen, Y. L. Niu, Y. R. Zhong, K. C. Zheng, B. H. Ye, *Inorg. Chem.* 2007, 46, 6427-6436.
- [39] (a) S. Das, S. Karmakar, S. Mardanya, S. Baitalik, *Dalton Trans.* 2014, 43, 3767-3782; (b) B. Chowdhury, S. Khatua, R. Dutta, S. Chakraborty, P. Ghosh, *Inorg. Chem.* 2014, 53, 8061-8070; (c) A. Paul, M. Bar, T. Ahmed, S. Baitalik, *Polyhedron* 2020, 190, 12; (d) T. K. Ghosh, S. Mondal, S. Bej, M. Nandi, P. Ghosh, *Dalton Trans.* 2019, 48, 4538-4546.
- [40] S. Mardanya, S. Karmakar, D. Maity, S. Baitalik, *Inorg. Chem.* **2015**, *54*, 513-526.
- [41] (a) T. K. Ghosh, S. Chakraborty, B. Chowdhury, P. Ghosh, *Inorg. Chem.* **2017**, *56*, 5371-5382; (b) T. K. Ghosh, P. Ghosh, *Dalton Trans.* **2018**, *47*, 7561-7570.
- [42] B. Sen, S. K. Patra, M. Rabha, S. K. Sheet, K. Aguan, D. Samanta, S. Khatua, *Eur. J. Inorg. Chem.* **2021**, 3549-3560.
- [43] (a) B. Chowdhury, S. Sinha, P. Ghosh, *Chem. Eur. J.* 2016, 22, 18051-18059; (b) S. Mondal, T. K. Ghosh, B. Chowdhury, P. Ghosh, *Inorg. Chem.* 2019, 58, 15993-16003.
- [44] M. Rabha, B. Sen, S. K. Sheet, K. Aquan, S. Khatua, *Dalton Trans.* **2022**, *51*, 11372-11380.
- [45] (a) C. B. Spillane, N. C. Fletcher, S. M. Rountree, H. van den Berg, S. Chanduloy, J. L. Morgan, F. R. Keene, J. Biol. Inorg. Chem. 2007, 12, 797-807; (b) C. B. Spillane, J. L. Morgan, N. C. Fletcher, F. R. Keene, J. G. Collins, Dalton Trans. 2006, 3122-3133; (c) C. B. Spillane, M. N. V. Dabo, N. C. Fletcher, J. L. Morgan, F. R. Keene, I. Haq, N. J. Buurmac, J. Inorg. Biochem. 2008, 10, 673–683.
- [46] C. B. Spillane, Queen's University, Belfast 2005.
- [47] E. C. Constable, K. R. Seddon, Chem. Commun. 1982, 34-36.
- [48] K. Suzuki, A. Kobayashi, S. Kaneko, K. Takehira, T. Yoshihara, H. Ishida, Y. Shiina, S. Oishic, S. Tobita, *Phys. Chem. Chem. Phys.* **2009**, *11*, 9850-9860.
- [49] E. Wolcan, G. Torchia, J. Tocho, O. E. Piro, P. Juliarena, G. Ruiz, M. R. Feliz, *J. Chem. Soc. Dalton Trans.* **2002**, 2194-2202.
- [50] L. Sacksteder, A. P. Zipp, E. A. Brown, J. Streich, J. N. Demas, B. A. DeGraff, *Inorg. Chem.* 1990, 29, 4335-4340.
- [51] Y. Ohsawa, S. Sprouse, K. A. King, M. K. DeArmond, K. W. Hanck, R. J. Watts, *J. Phys. Chem.* **1987**, *91*, 1047-1054.
- [52] M. A. Saeed, F. R. Fronczek, M. A. Hossain, Chem. Commun. 2009, 6409-6411.
- [53] M. J. Hynes, J. Chem. Soc., Dalton Trans., 1993, 311-312.
- [54] Gaussian 09, Revision E.01, M. J. Frisch, G. W. Trucks, H. B. Schlegel, G. E. Scuseria, M. A. Robb, J. R. Cheeseman, G. Scalmani, V. Barone, B. Mennucci, G. A. Petersson, H. Nakatsuji, M. Caricato, X. Li, H. P. Hratchian, A. F. Izmaylov, J. Bloino, G. Zheng, J. L. Sonnenberg, M. Hada, M. Ehara, K. Toyota, R. Fukuda, J. Hasegawa, M. Ishida, T. Nakajima, Y. Honda, O. Kitao, H. Nakai, T. Vreven, J. A. Montgomery Jr, J. E. Peralta, F.

- Ogliaro, M. Bearpark, J. J. Heyd, E. Brothers, K. N. Kudin, V. N. Staroverov, T. Keith, R. Kobayashi, J. Normand, K. Raghavachari, A. Rendell, J. C. Burant, S. S. Iyengar, J. Tomasi, M. Cossi, N. Rega, J. M. Millam, M. Klene, J. E. Knox, J. B. Cross, V. Bakken, C. Adamo, J. Jaramillo, R. Gomperts, R. E. Stratmann, O. Yazyev, A. J. Austin, R. Cammi, C. Pomelli, J. W. Ochterski, R. L. Martin, K. K. Morokuma, V. G. Zakrzewski, G. A. Voth, P. Salvador, J. J. Dannenberg, S. Dapprich, A. D. Daniels, O. Farkas, J. B. Foresman, J. V. Ortiz, J. Cioslowski, D. J. Fox, Gaussian, Inc., Wallingford CT, **2013**.
- [55] (a) Avogadro: an open-source molecular builder and visualization tool. Version 1.2.0, http://avogadro.cc/, 2016; (b) M. D. Hanwell, E. D. Curtis, D. C. Lonie, T. Vandermeersch, E. Zurek, G. R. Hutchison, J. Cheminform 2012, 4, 17.
- [56] P. A. Lay, A. M. Sargeson, H. Taube, *Inorg. Synth.* **1986**, *24*, 291-299.
- [57] N. A. F. Al-Rawashdeh, S. Chatterjee, J. A. Krause, W. B. Connick, *Inorg. Chem.* **2014**, *53*, 294-307.
- [58] M. Nonoyama, Bull. Chem. Soc. Jap. 1974, 47, 767-768.
- [59] J. Muldoon, A. E. Ashcroft, A. J. Wilson, Chem. Eur. J. 2010, 16, 100-103.
- [60] O. V. Dolomanov, L. J. Bourhis, R. J. Gildea, J. A. K. Howard, H. Puschmann, J. Appl. Crystallogr. 2009, 42, 339-341.
- [61] G. M. Sheldrick, Acta Crystallogr. Sect. A 2015, 71, 3-8.
- [62] G. M. Sheldrick, Acta Crystallogr. Sect. A 2008, 64, 112-122.